X-Ray Metrology for Quality Assurance

A. Noble, R. Hartley, J. Mundy and J. Farley
GE Corporate Research & Development
Schenectady, NY 12301

Abstract

There is considerable current interest in deriving accurate dimensional measurements of the internal geometry of complex manufactured parts, particularly castings. This paper describes an approach to the reconstruction of 3D part geometry from multiple digital X-ray images. A novel method for radiographic stereo is described which takes into account the special imaging geometry of the digital X-ray sensor modeled by a linear moving array, or pushbroom, camera. The 3D reconstruction algorithm employs a nominal geometric model which is perturbed by X-ray image constraints. Manufacturing applications are discussed and illustrated by experimental results on synthetic phantoms and actual casting images.

1 Introduction

Investment casting designs, particularly airfoils for aircraft engines and gas turbines, are rapidly evolving in complexity. In order to reduce the development cycle for a new design it is necessary to monitor and control the critical dimensions of the casting and associated cores and molds. In addition, detailed knowledge of the casting geometry is necessary to plan the drilling of cooling holes during airfoil manufacturing. We describe a new approach to dimensional control of casting machining operations based on X-ray metrology. Precise measurements of casting dimensions and hole geometry can be achieved using a new algorithm for radiographic stereo.

The most common form of X-ray image is a 2D digital radiographic (DR) image formed by the projection of rays from an x-ray point source on to a linear array of detectors (figure 1). 3D material density is projected to a 2D image as a line integral which can be directly related to material thickness (assuming that imaging parameters such as the point spread function of the imaging system and beam-hardening correction are known). However, in practice these parameters are not known precisely and only *relative* measurements can be made. Thus, industrial inspection from a single DR image has been largely limited to material flaw detection and part screening where the goal is to locate (local) abnormalities such as cracks, voids, or splatter from a laser, by looking for unexpected material density changes in otherwise uniform material density regions [1, 2, 3, 4].

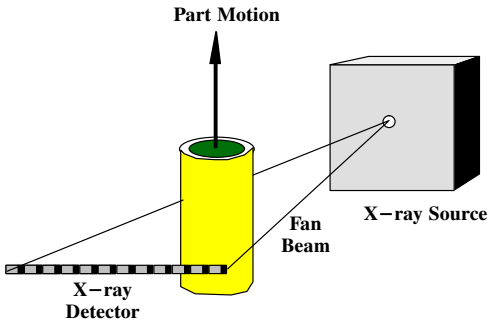

Figure 1. *Scanning geometry.*

A widely used method for internal part geometry verification is based on 2D computed tomography (2DCT) image analysis and many publications describing dimensional measurement algorithms from 2DCT have appeared in both the medical and NDE (nondestructive evaluation) literature, e.g. [5, 6]. 2DCT provides a slice-by-slice view of the internal geometry of a part [7, 8, 9]. Slices can be stacked on top of each other to provide a volumetric representation of a part (typically with interpolation between the slices to give an object a smoother appearance). However, this type of reconstruction requires a large amount of data to be analyzed and data acquisition is slow. Therefore it can not be used in near real-time applications such as process monitoring or high volume part inspection. Further, in many applications, a full volumetric analysis of an object (industrial or human) is not necessarily the desired final output. This is particularly true when the goal is to perform dimensional analysis and/or control where analysis typically only involves boundaries of the object.

In this paper we consider 3D geometry reconstruction from multiple view X-ray images as a means

to achieve practical 3D geometry measurement. Although CT reconstruction from a few views is ill-conditioned [10], one can, in theory, achieve it from a limited number of views of the object using *assumptions* about the geometry of the features being reconstructed, X-ray imaging distortions, and feature-based stereo reconstruction techniques. In the medical domain, this approach has been applied to estimate artery structure from biplane angiograms (2 views taken at 90 degrees apart) with some success. Here, the primary emphasis has been on the evaluation of the precision of boundary extraction techniques from 2D X-ray images to provide features for matching and reconstruction [11, 5, 12] modelling arteries (including bifurcations) and, the recovery of the 3D medial axes of arterial structures [13, 14].

This contribution presents a novel approach to 3D reconstruction from multiple views based on a linear pushbroom camera which is a simplified version of the pushbroom camera often used in photogrammetry to analyze satellite imagery [15]. In most previous work on multiple view X-ray reconstruction, affine (parallel projection) geometry has been assumed which is a good approximation to perspective (pinhole camera) geometry if the source-to-object distance is much larger than the depth of the object. A linear pushbroom camera, however, generates an image that can be considered as a projective image in one direction and an orthographic image in the other [16]. This more accurately captures the imaging geometry of a real X-ray system than an affine or perspective camera model. To our knowledge, this paper presents the first application of the linear-pushbroom camera model to feature-based stereo reconstruction. It also reports on the first application of multiple view X-ray reconstruction to industrial part inspection.

2 Approach

2.1 X-ray Imaging Scanning Geometry

The scanning geometry is depicted in Fig 1. A source projects X-rays through the part onto a linear array of sensors. The plane defined by the X-ray source and the sensor array is known as the *sensor plane*. A complete image is captured by moving the part by a series of step motions in a direction perpendicular to the sensor plane and capturing a new line of image data at each step. Subsequent images are captured in the same way after rotating the part through known angles about an axis perpendicular to the sensor plane.

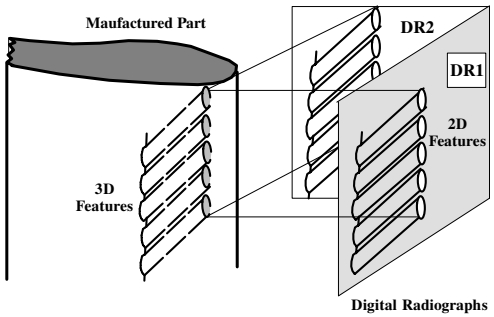

Figure 2. *Feature projection.*

2.2 Feature and Intensity Modeling

We consider the recovery of 3D drilled hole geometry from 2D X-ray projection images. We assume that drilled holes can be represented as right cylinders with elliptical cross-sections . It can be shown [17] that (under parallel projection) the projected thickness of a feature is also elliptic and the silhouette outlines of straight drilled holes are projected to straight lines as illustrated in figure 2. In a real DR image holes appear as dark elongated features as shown in figure 6.

The challenge in feature-based reconstruction is to extract features from several images taken at known (relative) view angles, establish the correspondence between the features in the views and recover the 3D geometry. We focus on the latter in the next section. Intensity feature modeling and template-based view correspondence are subjects of our current research (see the last section 4).

2.3 Object Reconstruction

The imaging geometry is shown in figure 3. We define a Euclidean coordinate frame as follows. The source is located at the origin. The y and z axes lie in the sensor plane, the z-axis (or *principal axis*) being perpendicular to the sensor array, and the y axis parallel to it. The x axis is perpendicular to the sensor plane, completing a right-handed coordinate system.

A mathematical model has been developed for this sort of imaging geometry, the linear-pushbroom model [16]. Let $(x, y, z)^T$ be the coordinates of a point in the part at time $t = 0$, the time when the first line is captured. The coordinates of the corresponding image point are $(u, v) = (u', v'/w')$ where

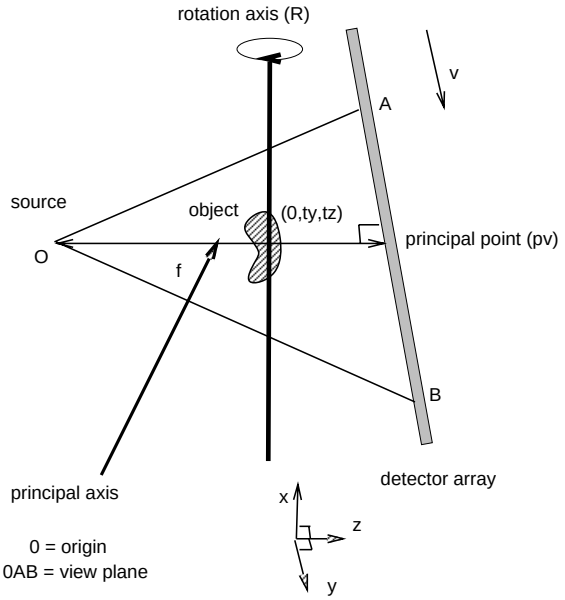

Figure 3. *Imaging geometry.*

$$\begin{pmatrix} u' \\ v' \\ w' \end{pmatrix} = \begin{pmatrix} 1 & 0 & 0 \\ 0 & f & p_v \\ 0 & 0 & 1 \end{pmatrix} \begin{pmatrix} 1/V_x & 0 & 0 \\ -V_y/V_x & 1 & 0 \\ -V_z/V_x & 0 & 1 \end{pmatrix} \begin{pmatrix} x \\ y \\ z \end{pmatrix}, \tag{1}$$

1. f is the focal length, that is, the distance from the origin to the sensor array along the z axis;

2. p_v is the coordinate of the principal point;

3. (V_x, V_y, V_z) is the motion vector of the part between scan lines of the image. Components V_z and V_y will nominally equal zero, corresponding to motion perpendicular to the sensor plane.

4. w' is a scale factor.

Separate Views : For each separate image, the part is rotated about an axis nominally perpendicular to the sensor plane. This rotation may be parametrized by the following parameters :

1. its angle θ_x;

2. the coordinates (t_y, t_z) of the point where the rotation axis meets the sensor plane;

3. two angles ϕ_y and ϕ_z determining the orientation of the rotation axis with respect to the perpendicular to the view plane. Nominally, these two angles are zero.

In terms of these parameters, it is possible to compute a 4×4 matrix R such that $(x', y', z', 1)^\top = R(x, y, z, 1)$, where $(x', y', z')^\top$ are the Euclidean coordinates of a point in the rotated part, and $(x, y, z)^\top$ are coordinates of the same point prior to rotation. Putting this together in equation 1 we find that

$$(u, vw, v)^\top = M(x, y, z, 1)^\top,$$

where $M = M_{f,p_v,V_x,V_y,V_z,\theta_x,t_y,t_z,\phi_y,\phi_z}$ is a 3×4 projection matrix depending on all the parameters.

Constraints : Though parameters V_y, V_z, ϕ_y and ϕ_z are nominally zero, there may be slight inaccuracies which cause them to deviate from their ideal values. In modeling the imaging process we assume these parameters as Gaussian random variables with zero mean and a small variance (see [13] for justification of this assumption). The other model parameters have known values and will similarly be modeled as random variables with appropriately chosen variances reflecting the degree of confidence in their nominal values. All model parameters except the rotation angle θ_x may be assumed to take the same values for all the images.

2.4 Reconstruction

Suppose we know the coordinates $\mathbf{u}^i$ of the image of a point $\mathbf{x}$ in a part being inspected, as seen in several views. As long as the camera parameters are known, $\mathbf{x}$ may in principle be computed as the intersection of the rays corresponding to all $\mathbf{u}^i$. If there are errors in the measurements of the $\mathbf{u}^i$, then the rays will not intersect exactly, and it will be necessary to compute a best fit to the intersection. Commonly, however, there may also be uncertainties in the modeling parameters. In this case, reconstructing $\mathbf{x}$ requires weighing the uncertainties in the modeling parameters against the uncertainties in the image coordinate measurements to estimate the most likely point position.

As seen in section 2.3, the mapping from 3D points to image points may be expressed as a function $F_{p_1 p_2 \ldots p_N}$ from R^3 (the 3D object space) to R^2 (the image), parametrized by a set of *model parameters* $p_1, p_2, \ldots, p_N$. Suppose we are given point correspondences $\mathbf{u}^i_j$, each of which is the image of an unknown point $\mathbf{x}_j$ as seen in image number i. We estimate $\mathbf{x}_j$ and p^i_k for each of the views so as to minimize a certain penalty function. Here p^i_k is the kth parameter of the ith view. Let $\hat{\mathbf{u}}^i_j = F_{p^i_1 p^i_2 \ldots p^i_N}(\mathbf{x}_j)$ be the image of the point $\mathbf{x}_j$ as seen in the ith view with the given calibration. Furthermore, let $\hat{p}^i_k$ be *a priori* estimations of the values of the modelling parameters.

The penalty function to be minimized is

$$\sum_{i,j} w_j^i ||\mathbf{u}_j^i - \hat{\mathbf{u}}_j^i||^2 + \sum_{i,k} v_k^i (p_k^i - \hat{p}_k^i)^2 \qquad (2)$$

where $1/(w_j^i)$ is the variance in the measurement of $\mathbf{u}_j^i$ and $1/(v_k^i)$ is the variance associated with the *a priori* estimates of the parameters p_k^i.

This estimation problem is solved using the Levenberg-Marquardt [18] parameter estimation algorithm. In this method, an initial guess at the values of the parameters is refined by iteration to reach a final least-squares estimate optimizing equation 2. At each step of the iteration, an adjustment to the values of the active variables is computed under an assumption of local linearity. If the modelling parameters are known with moderate accuracy, as is the case with an X-ray inspection system imaging setup, then the convergence is rapid from any initial estimate of the points $\mathbf{x}_j$.

2.5 Registering two 3D point sets

We next address the problem of registering two point sets $\{\mathbf{x}_j\}$ and $\{\mathbf{x}'_j\}$ in R^3 . In particular, we assume that the points are related by an unknown 3D similarity transformation, T, that is, the composition of a rotation, translation and isotropic scaling. The goal is to compute T. Since in the presence of noise one can not expect an exact fit, one seeks instead an optimal least-squares solution. In particular, we seek a similarity transformation T that minimizes the error

$$\sum_j ||\mathbf{x}_j - T\mathbf{x}'_j||^2 \qquad (3)$$

An efficient algorithm for computing the T that minimizes this term was given by Horn [19]. This algorithm uses quaternions to represent the unknown rotation [20], leading to a non-iterative rapid solution.

3 Experimental Results

In this section we present results of 3D geometry reconstruction using the approach outlined in the previous section. Synthetic data was produced using a fan-beam geometry phantom projection generation algorithm from a CT reconstruction software package written in C and implemented on a Meiko parallel processing system. Experimental X-ray images from real parts were provided by GE Aircraft Engines.

3.1 Hole pattern phantom

First, we consider the reconstruction of a synthetic drilled hole pattern which consists of 2 perpendicular rows of 5 cylindrical holes. Projection images were generated at 10^o intervals. Six views of a drilled hole pattern phantom are shown in figure 4. Relevant imaging geometry parameters are given in table 1. Features used in this experiment were the ends of the holes and feature selection and correspondence were established manually.

A good method of showing the accuracy of multiple-view reconstruction is to compute the 3D geometry using several views, reproject the result into a new view and compare how well the true and estimated features match. As an example, 3D hole geometry was estimated using stereo-reconstruction from the two views at angles 0^o and 30^o (figure 5). The 3D point estimates were then reprojected back into a third view at angle 60^o. The third image in figure 5 shows the result superimposed on the actual 60^o angle projection image. The agreement is very good.

3.2 Real Parts

Next, we show our approach applied to the reconstruction of 3D geometry for a real industrial part. We did not have a ground truth to compare our reconstruction results against (eg. a CAD model) so (as in the previous example) we chose to measure reconstruction accuracy *qualitatively* in terms of the observed accuracy of feature localization after reprojection of reconstructed 3D locations back into a view that was not used in the initial reconstruction.

Two X-ray views of the part are shown in figure 6 together with the features selected to perform the 3D reconstruction. The reprojected features computed after first reconstructing the 3D geometry and then reprojecting into a third view are shown superimposed on the actual projection image for this view. The agreement can be seen to be quite good.

To give an idea of part-to-part 3D measurement variability we computed the estimated mean and standard deviation of hole length (in 3D) for 5 industrial parts using our approach. The same view angles and image features were used for each reconstruction. The results are summarized in table 2 and show that drilled hole lengths have fairly good repeatability across parts. Some of the variability can be explained as being due to the use of manual rather than automatic feature selection (measurement error) and another key source is manufacturing process variability.

We plan to compare the accuracy of reconstruction against available CAD models and physical dimensions computed by cutting up manufactured parts in the near future.

Table 1. Imaging geometry parameters.

θ_x	detect. spacing	pixel size	central detect. pos.	**OC**	**0P**	image height (y)	image width (x)
10^o	$0.00575''$	$0.005''$	128	$17.132''$	$14.47''$	110 pixels	256 pixels

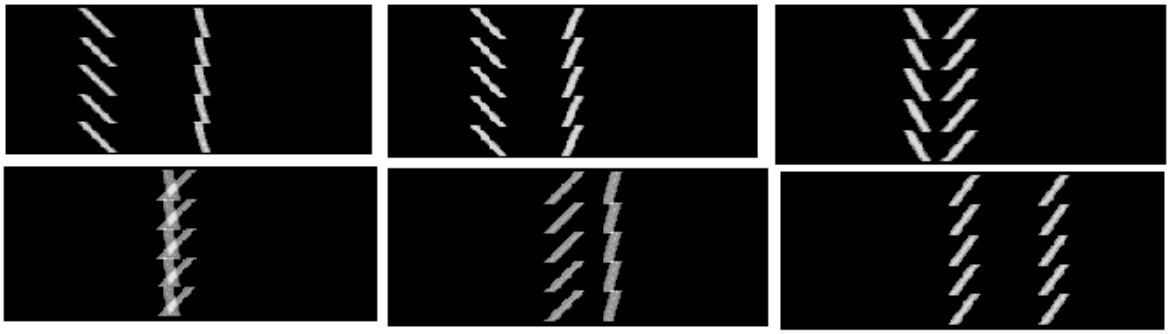

Figure 4. *Views of a drilled hole pattern phantom at angles* $30, 70, 100, 120, 140$ *and* 170 *degrees.*

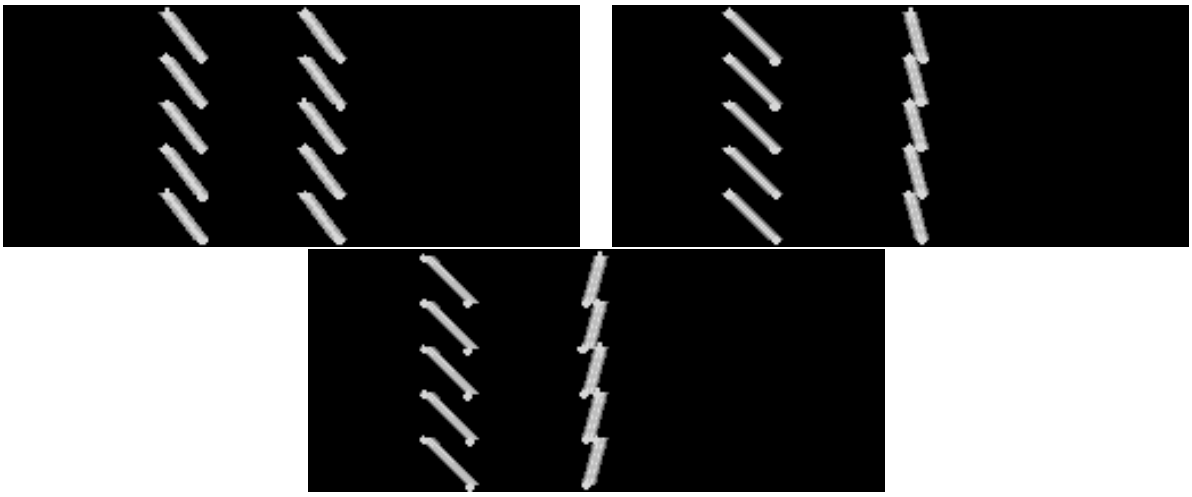

Figure 5. *Two views used for reconstruction and the reprojection into a third view.*

hole	mean	variance
0	45.4571	5.76908
1	55.4283	10.8301
2	58.3581	9.67349
3	55.1082	8.05943
4	59.9354	17.4874

Table 2. *3D hole length statistics computed from multiple view X-ray reconstruction for 5 industrial parts.*

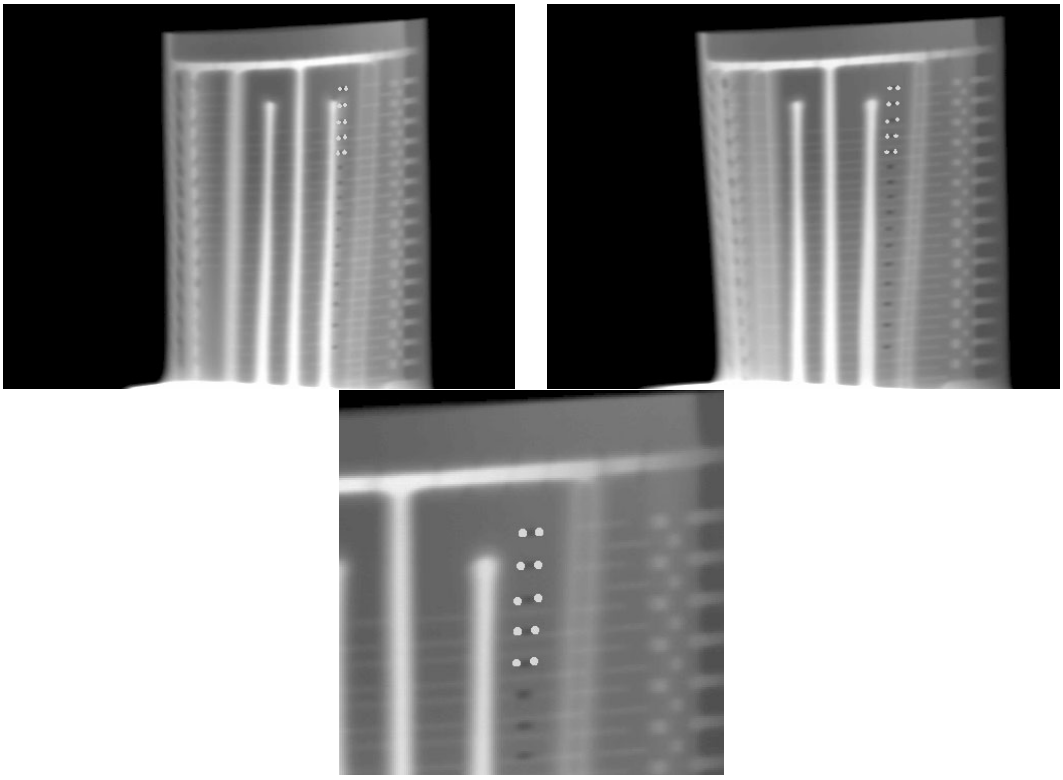

Figure 6. *Two views of a real part used for reconstruction and the reprojection into a third view.*

4 Future Work

We have described a new approach to 3D geometry reconstruction from multiple 2D X-ray images and presented experimental results on X-ray data from synthetic phantoms and real industrial parts. A key practical advantage of our approach over volumetric CT reconstruction is that both data acquisition and reconstruction times are fast. However, much work still needs to be done to evaluate the precision of internal geometry measurement achievable with this approach in order to demonstrate the practical use of multiple view X-ray reconstruction.

There are a number of directions in which this work could be extended.

- Automation - the results in this paper were achieved using manual feature selection and correspondence. We are currently working on template-based feature extraction and registration methods to automate these two steps.
- Fine stereo-reconstruction - our approach provides a way to determine the 3D geometry of a part using a global "best-fit" to a set of feature points. In many cases, high precision measurement on individual features is also desired - for example the maximum radius along a laser-drilled hole. This could be achieved by initially performing feature-based geometry estimation using the approach described in this paper and then refining the geometry estimate by nonlinear optimization of a combined intensity and geometry representation of part feature that accounts for X-ray imaging effects and noise. We refer to these two stages as coarse and fine multiple view X-ray stereo-reconstruction. We plan to investigate this approach in future work.
- Precision measurement integration - Another interesting question is how internal geometry measurements derived from X-ray-based reconstruction can be combined with surface profile measurements derived, for example, from coordinate measurement machines, laser profile scanning and optical images to provide an integrated data representation of a manufactured part. Many areas of manufacturing design (for example tolerancing [21, 22] and engineering analysis) and inspection (for example automated inspection planning [23]) would benefit from the availability of information of this kind.

Acknowledgements

We thank David Johnson for collecting experimental data, Meng-ling Hsiao for the use of the phantom generation software and Jean Ponce for comments on the paper.

References

[1] H. Decker. A Difference Technique for Automatic Inspection of Casting Parts. Pattern Recognition Letters, vol. 2, pages 125-129, 1983.

[2] H. Strecker. A Local Feature Method for the Detection of Flaws in Automated X-Ray Inspection of Castings. Signal Processing, vol. 5, pages 423-431, 1983.

[3] H.Boerner, and H. Strecker. Automated X-Ray Inspection of Aluminum Castings. IEEE PAMI, vol 10, no. 1, pages 79-91, 1988.

[4] A. Noble, V.D. Nguyen, C. Marinos, et al. Template Guided Visual Inspection. ECCV, Santa Margherita, Italy, pages 893-901, 1992.

[5] T.N. Pappas and J.S. Lim. A New Method for Estimation of Coronary Artery Dimensions in Angiograms. IEEE ASSP, vol. 36, no. 9, pages 840-858, 1988.

[6] E. Segal, A. Notea and Y. Segal. Dimensional Information Through Industrial Computerized Tomography. Materials Evaluation, vol. 40,pages 1268-1272, 1982.

[7] H.J. Scudder. Introduction of Computer Aided Tomography. Proc. IEEE, vol. 66, pages 628-637, 1978.

[8] A. Kak. Computerized Tomography with X-rays, Emission, and Ultrasound Sources. Proc. IEEE, vol. 67, pages 1245-1272, 1979.

[9] A.C. Kak and M. Slaney. Principles of Computerized Tomographic Imaging. IEEE Press, New York NY, 1988.

[10] D.J. Rossi and A.S. Willsky. Reconstruction from Projections Based on Detection and Estimation of Objects - Part I and II. IEEE ASSP, vol. 32, no. 4,pages 886-906, 1984.

[11] K. Shmueli, W.R. Brody, and A. Macovski. Estimation of Blood Vessel Boundaries from X-ray Images. Opt. Eng., vol. 22, no. 1, pages 110-116, 1983.

[12] L.V. Tran and R.C. Bahn and J. Sklansky. Reconstructing the Cross Sections of Coronary Arteries from Biplane Angiograms. IEEE Trans. Med. Imaging, vol. 11, no. 4, pages 517-529, 1992.

[13] K. Kitamura, J. Tobis, and J. Sklansky. Estimating the 3D Skeletons and Transverse Areas of Coronary Arteries from Biplane Angiograms. IEEE Trans. Med. Imaging, vol 7, no 3, pages 173-187, 1988.

[14] Y. Bresler and J.A. Fessler and A. Macovski. A Bayesian Approach to Reconstruction from Incomplete Projections of a Multiple Object 3D Domain. IEEE PAMI, vol. 11, no. 8, pages 840-858, 1989.

[15] American Society of Photogrammetry. Manual of Photogrammetry. Edition 4, Fall Church, VA.

[16] R. Hartley and R. Gupta. Linear Pushbroom Cameras. Accepted to the 1994 European Conference on Computer Vision.

[17] A. Rosenfeld and A.C. Kak. Digital Picture Processing. Academic Press, London, 1982.

[18] W.H. Press, B.P. Flannery, S.A. Teukolsky, and W.T.Vetterling. Numerical Recipes in C: The Art of Scientific Computing. C.U.P., 1988.

[19] B.K.P. Horn, Relative Orientation Revisited. J. Opt. Soc. Amer., A vol. 8, no. 10, pages 1630-1638, 1991.

[20] O.D. Faugeras and M. Hebert. The Representation, Recognition, and Locating of 3D Objects. Int. J. Robot. Res., vol 5, no 3, pages 27-52, 1986.

[21] D.C. Gossard, R.P. Zuffante and H. Sakuria. Representing Dimensions,Tolerances and Features in MCAE Systems. IEEE Comp. Graphics Applic., pages 51-59, 1988.

[22] A.A.G. Requicha. Toward a Theory of Geometric Tolerancing. Int. J. Robot. Res., vol 2, no 4, pages 45-60, 1983.

[23] A.J. Spyridi and A.A.G. Requicha. Automatic Programming of Coordinate Measuring Machines. Accepted to 1994 IEEE Int. Conf. Robotics & Automation.